

Investigation of Tensile Strength and Thermal Properties of Chitosan / PVA Blend Prepared at Different Ratios

Estabraq Hasan Rashed¹ and Hanaa Shuker Mahmood^{1*}

¹Department of Physics, College of Pure Science Ibn Alhatham, University of Baghdad, Baghdad, Iraq

*Corresponding author: hanaa.s.m@ihcoedu.uobaghdad.edu.iq

Abstract

In this study, chitosan/polyvinyl alcohol (CS/PVA) films were prepared with different weight ratios (98:2, 96:4, 94:6, 92:8, and 90:10%) using the solution casting method to study the structural, thermal, and tensile strength properties of the composites. The Fourier transform infrared (FTIR) spectroscopy of CS/PVA samples showed some differences, such as changes in the strength, location, and intensity of the CO and CH₂ stretching bands. The differential scanning calorimetry (DSC) revealed that the incorporation of PVA enhanced the thermal stability of the composites, with the 98:2wt.% blending the highest melting temperature (T_m) at 289°C. The thermogravimetric analysis (TGA) further confirmed improved thermal stability, showing a significant shift in the decomposition peak toward higher temperatures and reduced mass loss within the degradation zone (approximately 40 wt.% loss between 250 and 400°C). Mechanically, the CS/PVA 98/2 wt.% blend demonstrated optimal performance, achieving a tensile strength of 54.94 MPa, an elongation at break of 3.93%, and a Young's modulus of 1.48 GPa. Scanning electron microscopy (SEM) showed a highly homogeneous distribution of PVA within the chitosan at this specific ratio, directly correlating with the superior tensile strength and enhanced flexibility of the composite.

Article Info.

Keywords:

Chitosan, Blend,
Polyvinyl Alcohol(PVA),
Tensile Strength, DSC.

Article history:

Received: May, 11, 2025

Revised: Jun. 25, 2025

Accepted: Jul. 09, 2025

Published: Jun. 01, 2026

1. Introduction

Polymers are materials that are receiving increasing attention these days due to their applications in various fields. Polymers are used in everyday life, including as building materials, paper, clothing, fibres, and plastics, such as those used in the plastic and rubber industries, as well as in solar cells, batteries, and energy applications. Additionally, polymers are utilized in environmental and medical contexts due to their unique properties [1-5]. These materials have improved physical and chemical properties, and each can be applied individually in industrial fields [6]. They can be a polymer mixture specially designed to maintain specific properties. Natural and synthetic polymers offer an intriguing way to develop new materials [7].

The natural polymer chitosan (CS) occupies a special place due to its versatility; its medicinal value is enhanced by blending it with synthetic and natural polymers to expand its range of applications [8,9]. When chitosan is mixed with synthetic polymers such as polyvinyl alcohol (PVA), it increases its compatibility with living tissue, which is important for medical applications. It is considered the second most common type of chitin that occurs naturally in the shells of shrimp and crustaceans. The amino groups in the chitosan chain can be dissolved in dilute aqueous acid solutions, such as acetic acid. Being non-toxic and environmentally friendly, chitosan has functional groups such as the hydroxyl groups (OH) that help in the solubility of chitosan and improve its ability to form polymer films, and it has been evaluated for its numerous applications [10]. Polyvinyl alcohol is a water-soluble synthetic polymer. It has many hydroxyl groups, allowing it to interact with many types of functional groups, which makes this feature suitable as a biocompatible material. PVA has been widely used due to its biocompatibility and non-toxicity. It has been used in various fields, including industry and medical applications [11].

The objective of this study is to prepare a mixture of chitosan and PVA to produce a tissue-compatible biomaterial used as a dressing to promote and accelerate wound healing [12,13]. This study focuses on the structural properties, Young modulus, and thermal properties of biodegradable polymers. Through our findings, they can be used in medical applications such as wound healing [14].

2. Experimental Part

2.1. Preparation Samples

CS was blended with different PVA weight ratios (2, 4, 6, 8, 10 wt.%) to prepare the CS/PVA blends using the solution casting method. Table 1 shows the weights of CS and PVA used to prepare the different blend samples. To prepare six samples of different CS/PVA ratios, the CS solution was first prepared by dissolving the specified weight of chitosan in 50 mL of dilute acetic acid 1% in separate glass beakers using a magnetic stirrer at 300 rpm for 6 h at room temperature, with the material being added slowly until complete dissolution. The specified weight of additive PVA polymers was dissolved in 2 mL of distilled water in a small glass container using the magnetic stirrer, gradually at room temperature. PVA polymer solution was added dropwise to the prepared chitosan solution, gradually mixing until the sample material was completely blended and appeared miscible. Samples were prepared separately at different ratios. Fig. 1 shows the sample preparation models. The thickness of the mixture sample was measured at three locations for each sample using a manual micrometer. Fig. 2 shows the film samples of different mixing ratios of CS/PVA. The film thickness was approximately 0.2 mm for all samples.

Table 1: Sample ratio and its components' weights.

Symbols	CS wt.%	PVA wt.%
A1	98	2
A2	96	4
A3	94	6
A4	92	8
A5	90	10

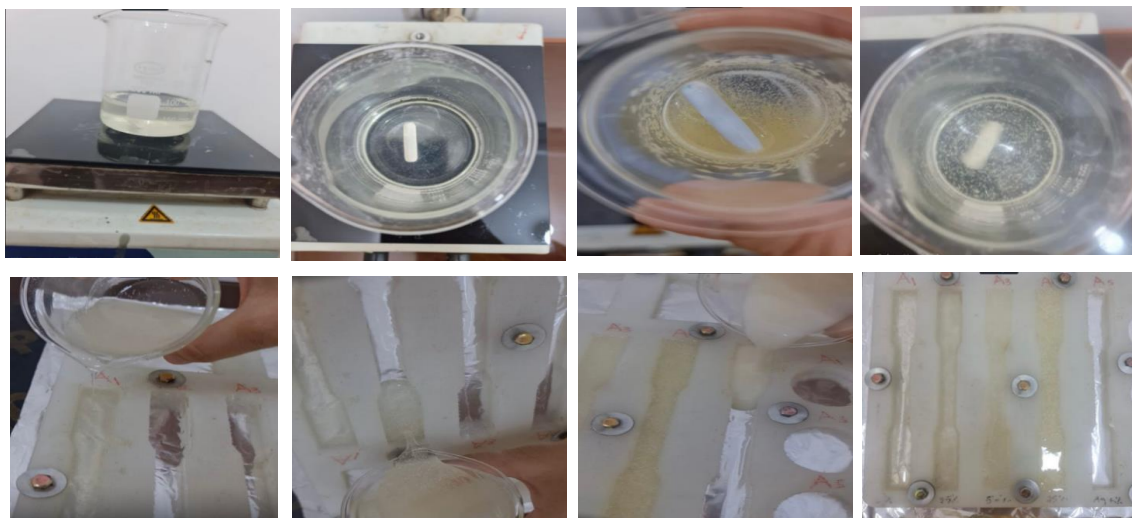


Figure 1: Sample preparation models.

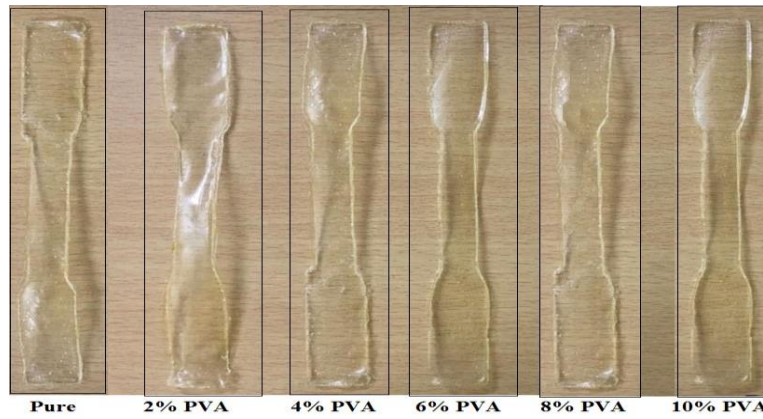


Figure 2: Film samples for different mixing ratios of CS:PVA.

3. Results and Discussion

3.1. Fourier-Transform Infrared Spectroscopy (FTIR)

The FTIR spectra for CS and CS/PVA blends are presented in Fig. 3. The CS powder stretching vibrations of the -OH bond was found at 3427.18 cm^{-1} . The absorption bands at 2912.27 and 2882.58 cm^{-1} belong to CH_2 stretching vibration. The peak at 1100.50 cm^{-1} corresponds to C-O stretching of amide I, and the band at 1680.55 cm^{-1} corresponds to the bending energy band in N-H bond of the amine group [15]. The deformation band for CH_2 appeared at 1471.15 cm^{-1} , and the small peak at 1325.22 cm^{-1} was assigned to the C-N stretching of (amide II) [16,17]. The small peak observed at 1661.36 cm^{-1} corresponds to C-O vibration. Most of the absorption bands in this sample belong to the polysaccharides, where the monosaccharide is the basic form of CS [18].

The characteristic of the C-O bands for chitosan shifts from 1829 to 1155.28 cm^{-1} . The intensity decreases due to the reduced oxidative activity of the glycosidic bond between polysaccharides. The absorption bands at 2935.22 and 2978.60 cm^{-1} belong to CH_2 stretching vibration. The symmetric and asymmetric CH_2 stretching bonds increase in intensity with increasing PVA ratios due to the formation of the blend. The peak shifting and some characteristic peak intensity variations are due to the blend formation and emergence of the hydroxyl bond between PVA and CS molecules belonging to the CH_2 stretching vibration. The intensity and location of the carbon dioxide and methane stretch bands were reduced. However, with the addition of polyvinyl alcohol, two peaks appeared, and these two peaks remained with the mixing of different proportions of PVA [19].

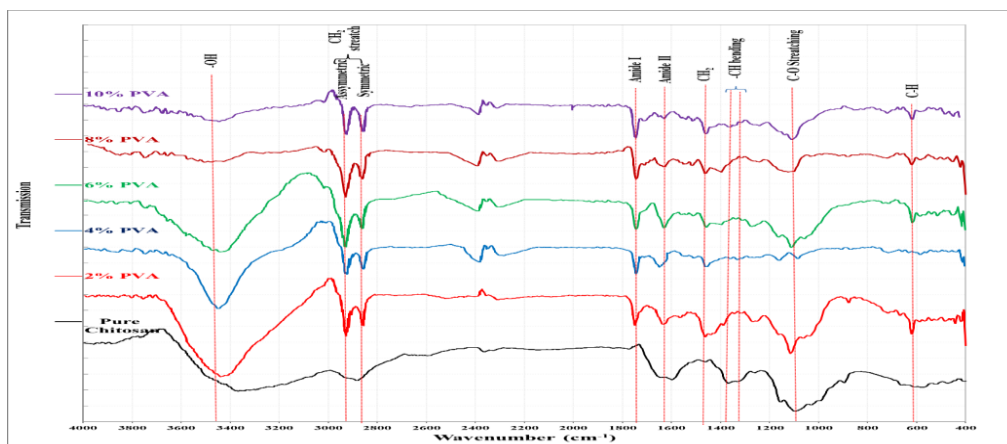


Figure 3: FTIR spectra of CS and CS/PVA blends at different ratios.

3.2 Scanning Electron Microscope (SEM)

Fig. 4 illustrates the SEM images (with magnification powers of $\times 30$ k) of the surface of the CS/PVA (98:2wt.%) blend. The images indicated that both mixtures had good miscibility and formed a homogeneous mixture. This is due to the good mixing of chitosan and PVA, which leads to a cohesive network of polymer chains. This is reflected in the images as an interlocking structure with no obvious voids [20].

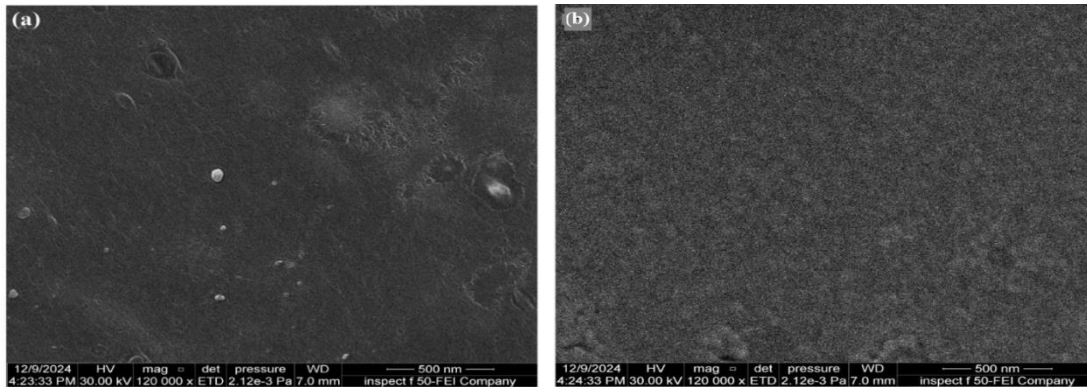


Figure 4: SEM images (a) pure CS and (b) for CS/PVA (98:2) blend.

3.3. Thermal Analysis

Fig. 5 shows the differential scanning calorimetry (DSC) patterns of a pure chitosan and CS/PVA blend samples at a heating rate of $10\text{ }^{\circ}\text{C}/\text{min}$ in an argon atmosphere. The broad peak in the DSC pattern of the pure chitosan sample at $107.6\text{ }^{\circ}\text{C}$ is attributed to the loss of water from the sample due to the energy required for the water dehydration process. The broad peak and its high-water resistance indicate that chitosan has properties binding it strongly to water. At the starting point of $244\text{ }^{\circ}\text{C}$, the DSC curve was observed. The highest exothermic peaks appeared at $280\text{ }^{\circ}\text{C}$, indicating the chitosan decomposition at this temperature [21]. It was shown that at a temperature of $244\text{ }^{\circ}\text{C}$, CS maintains the thermal stability and properties it possesses after mixing it with PVA in different ratios. It was also observed that there were no thermal changes [24], indicating increased thermal stability of the mixture. This can be attributed to the subsequent miscibility and bonding between chitosan and PVA. After the temperature reaches more than $244\text{ }^{\circ}\text{C}$, as the proportion of polyvinyl alcohol increases, the mixture begins to decompose. Mixing CS/PVA leads to differences in thermal stability. Both CS/PVA are hydrophilic. This shows that the proportion of water in the mixture is high. The endothermic water drying peak at about $125\text{ }^{\circ}\text{C}$ appeared more intense for the mixture samples. This is because CS/PVA has strong bonds with water molecules, which decompose the material and require high energy. The glass transition temperature is $145\text{ }^{\circ}\text{C}$ [22].

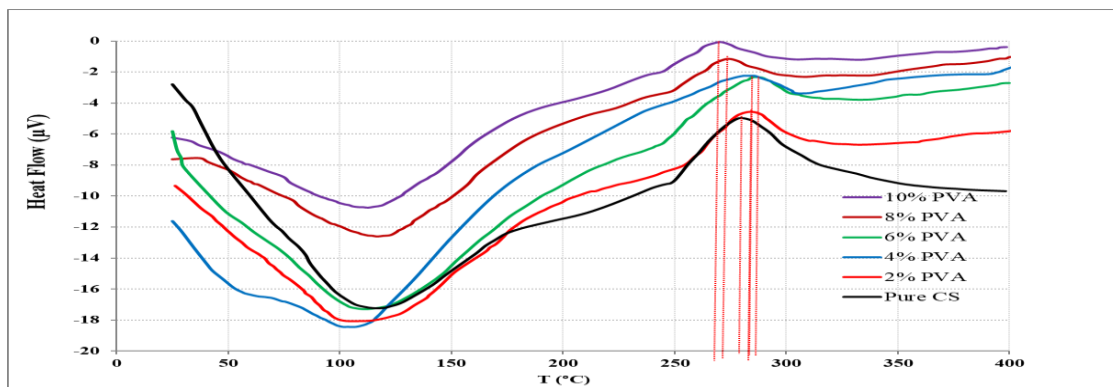


Figure 5: The DSC curves of CS/PVA at different CS/PVA blend ratios.

3.4. Thermogravimetric Analysis (TGA)

TGA curves for the pure CS and CS/PVA blend samples of different ratios are shown in Fig. 6. They show that the mass loss of the mixture samples when heated to 250°C begins with the decomposition of chitosan and the sugar rings in chitosan, and the carbon bonds in PVA begin to break, showing a clear mass loss. About 40% of the mass was at temperatures ranging from 250 to 330 °C. However, the addition of PVA has changed the properties of the resulting polymer. The composite blend CS/PVA in the ratio (98:2wt.%) shows the best heat stability. This can be explained by the fact that the 2% ratio leads to the formation of sufficient hydrogen bonds between the OH-NH₂ group in chitosan and the OH group in PVA, which reduces the movement of the molecular chains and enhances the cohesion of the crystal structure.

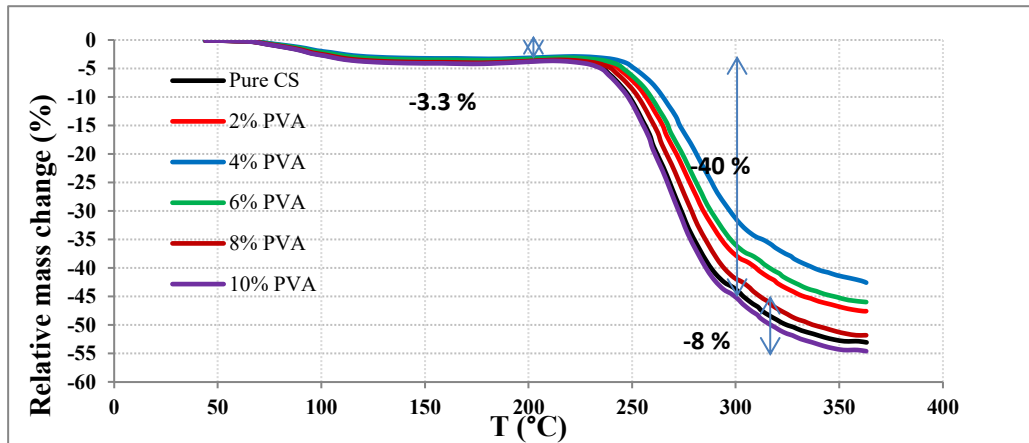


Figure 6: The TGA curves of CS/PVA blends at different CS/PVA ratios.

3.5. Tensile Strength

Fig. 7 shows the stress-strain curves for CS and CS/PVA blends. The blending process involves mixing two polymers by casting them into a weight ratio of PVA. The stress-strain curve of the mixture shows a clear linear relationship in the elastic region according to Hooke's law. Fig. 7 illustrates the effect of the mechanical properties of polymers on hydrogen bonding. It is noted that the tensile strength increases with increasing the proportion of PVA in the mixture up to 2%, and decreases as the proportion increases. This is due to the formation of a bond between CS/PVA as a result of rigid hydrogen bonds between the OH groups of chitosan amine and the CS/PVA ether groups (CH₃) [23,24]. This indicates an increase in the flexibility of the mixture, which is linked to increased mobility of the polymer chains.

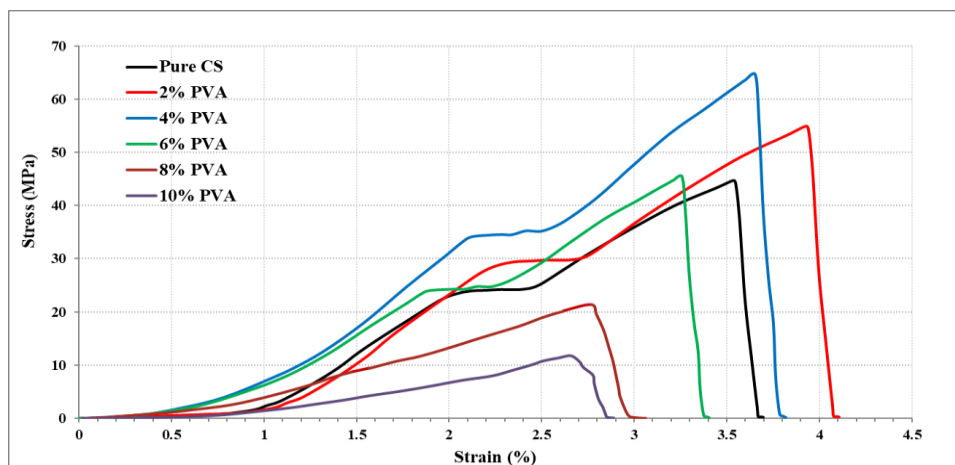


Figure 7: Stress-strain curves for CS/PVA blend at different PVA ratios.

Fig. 8 shows the stress-strain curves of CS and CS/PVA blend samples at different CS/PVA ratios. The modulus of elasticity is a measure of the material's stiffness, while the maximum elongation before break is a measure of the elasticity. The figure shows the variation of Young modulus and ultimate elongation of CS/PVA blends with the change of the PVA%. The maximum value of Young's modulus was 1.48 MPa at a 2% PVA. The maximum elongation was also enhanced by the same ratio, indicating that the CS/PVA ratio of 98:2 increased the flexibility of the sample, which is due to the strong hydrogen bonding between –OH and –NH₂ in chitosan and –OH groups in PVA. The combination of an appropriate Young's modulus value and a high elongation percentage in the chitosan/PVA blend reflects a mechanical balance between stiffness and flexibility, which is essential for biomaterials used in wound healing and tissue engineering. This balance allows the material to provide sufficient mechanical support to protect tissues [25]. Also, the increase in the small modulus in the optimized sample was explained by the enhancement of the mixture. Table 2 shows the highest Young modulus, maximum stress, and maximum strain for the CS/PVA blend at different CS/PVA ratios.

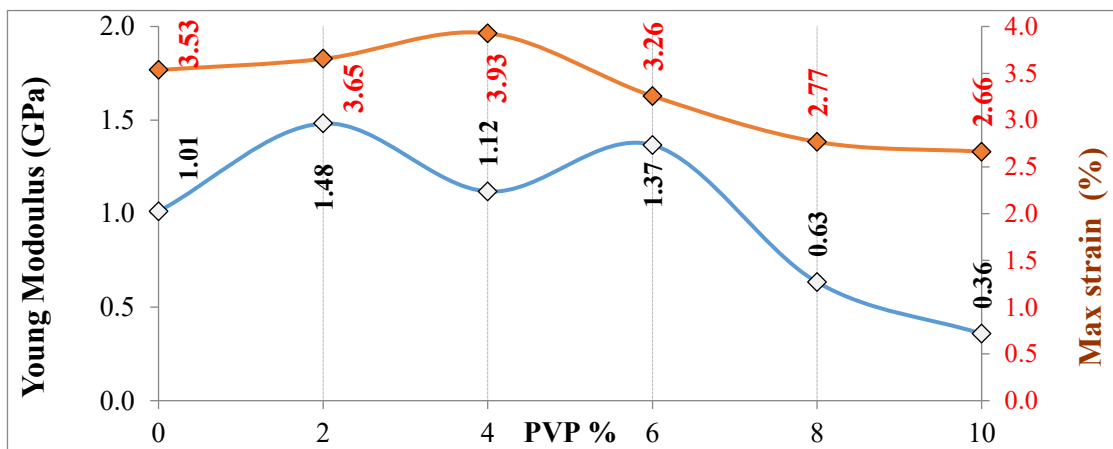


Figure 8: Stress and maximum strain for CS/PVA blend at different PVA%.

Table 2: The highest Young modulus, maximum stress, and maximum strain for CS/PVA blend at different PVA weight ratios.

Symbol	PVA wt. %	Max. Stress (MPa)	Max. Strain (%)	Young Modulus (GPa)
A	0	44.74	3.53	1.01
B	2	54.94	3.93	1.48
C	4	64.60	3.65	1.12
D	6	45.37	3.26	1.37
E	8	21.42	2.77	0.63
F	10	11.69	2.66	0.36

4. Conclusions

In this summary, this study successfully fabricated CS films reinforced with PVA using the solution casting technique. The experimental findings demonstrated that the structural, thermal, and mechanical properties of the composite films are highly dependent on the CS/PVA blending ratio. The comprehensive characterization revealed that the 98:2wt.% CS/PVA blend exhibits the most optimal performance, delivering superior thermal stability, a significant increase in Young's modulus, and enhanced tensile strength compared to the other formulations. FTIR and SEM analyses confirmed excellent intermolecular compatibility, a highly homogeneous surface texture, and uniform component distribution without any noticeable phase segregation or particle aggregation. These outstanding synergistic properties, combined with the inherent

biocompatibility of the base polymers, strongly support the potential utilization of the prepared CS/PVA composite films in advanced biomedical applications, specifically for effective wound dressing and high-quality surgical structures.

Conflict of Interest

The authors declare that they have no conflict of interest.

References

1. H. S. Mahmood and N. F. Habubi, Structural, mechanical and magnetic properties of PVA-PVP: iron oxide nanocomposite, *Appl. Phys. A*, **128**, 956 (2022). <https://doi.org/10.1007/s00339-022-06107-6>.
2. H. S. Mahmood and N. F. Habubi, in *Proceedings of the 3rd International Conference on Mathematics and Applied Science (ICMAS 2022)*, *Journal of Physics: Conference Series*, 2022, p. 012068. <https://doi.org/10.1088/1742-6596/2322/1/012068>.
3. A. K. Azad, N. Sermsintham, S. Chandkrachang, and W. Stevens, Chitosan membrane as a wound-healing dressing: characterization and clinical application, *J. Biomed. Mater. Res. B Appl. Biomater.* **69**, 216 (2004). <https://doi.org/10.1002/jbm.b.30000>.
4. H. S. Mahmood and N. F. Habubi, Mechanical and antibacterial activity of biodegradable Na-CMC: PVA reinforced with Al₂O₃ nanoparticles, *Int. J. Nano Biomater.* **10**(4), 221 (2024). <https://doi.org/10.1504/IJNB.2024.143829>
5. C. Enrique, F. Armando, F. Bossard, and M. Rinaudo, Biomaterials Based on Electrospun Chitosan. Relation between Processing Conditions and Mechanical Properties, *Polym.* **10**(3), 257 (2018). <https://doi.org/10.3390/polym10030257>
6. A. Kucukgulmez, M. Celik, Y. Yanar, D. Sen, H. Polat, and A. E. Kadak, Physicochemical characterization of chitosan extracted from *Metapenaeus stebbingi* shells, *Food Chem.* **126**, 1144 (2011). <https://doi.org/10.1016/j.foodchem.2010.11.148>.
7. R. Santa, B. Rosa, V. Alexandre, R. Ícaro, E. Paloma, R. José, C. Andrés, and M. Vinícius, Preparation and Characterization of Chitosan Obtained from Shells of Shrimp (*Litopenaeus vannamei* Boone), *Mar. Drugs* **15**(5), 1 (2017). <https://doi.org/10.3390/md15050141>.
8. A. Escarcega, J. Cruz-Mercado, J. Lopez-Cervantes, O. Brito-Zurita, D. Sánchez-Machado, and J. M. Ornelas-Aguirre, Chitosan treatment for skin ulcers associated with diabetes, *Saudi J. Biol. Sci.* **25**, 1 (2018). <https://doi.org/10.1016/j.sjbs.2017.03.017>.
9. A. Kumar, A. Vimal, and A. Kumar, Why Chitosan? From properties to perspective of mucosal drug delivery, *Int. J. Biol. Macromol.* **91**, 615 (2016). <https://doi.org/10.1016/j.ijbiomac.2016.05.054>.
10. S. Hajji, N. Ktari, R. Ben Salah, S. Boufi, F. Debeaufort, and M. Nasri, Development of Nanocomposite Films Based on Chitosan and Gelatin Loaded with Chitosan-Tripolyphosphate Nanoparticles: Antioxidant Potentials and Applications in Wound Healing, *J. Polym. Environ.* **30**, 833 (2021). <https://doi.org/10.1007/s10924-021-02239-7>.
11. A. Oryan and S. Sahvich, Effectiveness of chitosan scaffold in skin, bone and cartilage healing, *Int. J. Biol. Macromol.* **104**, 1003 (2017). <https://doi.org/10.1016/j.ijbiomac.2017.06.124>.
12. C. Brown, Y. Li, J. Seelenbinder, P. Pivarnik, A. Rand, S V Letcher, O J Gregory and S. V. Letcher, Immunoassays based on surface-enhanced infrared absorption spectroscopy, *Anal. Chem.* **70**(14), 2991 (1998). <https://doi.org/10.1021/ac980058k>.
13. L. S. Casey and L. D. Wilson, Investigation of Chitosan-PVA Composite Films and Their Adsorption Properties, *J. Geosci. Environ. Prot.* **3**(2), 55214 (2015). <https://doi.org/10.4236/gep.2015.32013>.
14. A. Barzegari and Z. Shariatinia, Fabrication of Chitosan-Polyethylene Oxide Electrospun Nanofibrous Mats Containing Green Tea Extract, *Iran. J. Chem. Eng.* **15**(2), 65 (2018).
15. C. Song, H. Yu, M. Zhang, Y. Yang, and G. Zhang, Physicochemical properties and antioxidant activity of chitosan from the blowfly *Chrysomya megacephala* larvae, *Int. J. Biol. Macromol.* **60**, 347 (2013). <https://doi.org/10.1016/j.ijbiomac.2013.05.039>.
16. A. H. Shaffie and A. S. A. Khair, in *Proceedings of the AIP Conference Proceedings*, 2018, p. 030011. <https://doi.org/10.1063/1.5041232>.
17. E. Chiellini, H. Gil, G. Braunegg, J. Buchert, P. Gatenholm, and M. van der Zee, *Biorelated Polymers: Sustainable Polymer Science and Technology* (Springer Science, 2001). <https://doi.org/10.1007/978-1-4757-3374-7>.
18. S. D. Ray, Toxicological and pharmaceutical applications of biopolymers, *Acta Pol. Pharm.* **68**(5), 619 (2011).

19. R. Onnainty, B. Onida, P. Páez, M. Longhi, A. Barresi, and G. Granero, Targeted chitosan-based bionanocomposites for controlled oral mucosal delivery of chlorhexidine, *Int. J. Pharm.* **509**(1-2), 408 (2016). <https://doi.org/10.1016/j.ijpharm.2016.06.011>.
20. H. S. Mahmood and M. K. Jawad, Investigation of Chitosan/PEO Reinforced with AgNPs for Antibacterial Activity Prepared by Solution Casting Method, *Ann. Trop. Med. Public Health* **22**, 70 (2019). <https://doi.org/10.36295/ASRO.2019.220910>.
21. D. S. Lakshmi, S. Jaiswar, M. Saxena, F. Tasselli, and H. D. Raval, Preparation and performance of biofouling resistant PAN/chitosan hollow fiber membranes, *3 Biotech* **7**,224 (2017). <https://doi.org/10.1007/s13205-017-0798-2>.
22. J. Nunthanid, S. Puttipipatkachorn, K. Yamamoto, and G. E. Peck, Physical Properties and Molecular Behavior of Chitosan Films, *Drug Dev. Ind. Pharm.* **27**(2), 143, (2001). <https://doi.org/10.1081/DDC-100000481>.
23. L. Boone, R. Santa, C. Martins, D. Q. Antonino, B. Rosa, P. Lia, E. Paloma, N. Lima, R. José, C. Andrés, P. Covas, M. Vinicius, and L. Fook, Preparation and Characterization of Chitosan Obtained from Shells of Shrimp (*Litopenaeus vannamei* Boone), *Mar. Drugs* **15**(5), 1 (2017). <https://doi.org/10.3390/md15050141>.
24. F. Heidari, M. Razavi, M. E. Bahrololoom, R. B. Lari, D. Vashae, H. Kotturi and L. Tayebi, Mechanical Properties of Natural Chitosan/Hydroxyapatite/Magnetite Nanocomposites for Tissue Engineering Applications, *Mater. Sci. Eng. C* **65**, 338, (2016). <https://doi.org/10.1016/j.msec.2016.04.039>.
25. S. B. Qasim, M. S. Zafar, S. Najeeb, Z. Khurshid, A. H. Shah, S. Husain, and I. U. Rehman, Electrospinning of Chitosan-Based Solutions for Tissue Engineering and Regenerative Medicine, *Int. J. Mol. Sci.* **19**(2), (2018). <https://doi.org/10.3390/ijms190205>.

دراسة متانة الشد والخواص الحرارية لمزيج الكيتوزان/بولي فينيل الكحول المحضر بنسب مختلفة

استبرق حسن راشد¹ وهناء شكر محمود¹

¹تقسم الفيزياء، كلية العلوم الصرفة ابن الهيثم، جامعة بغداد، بغداد، العراق

الخلاصة

تم تحضير، في هذه الدراسة، أغشية من الكيتوزان/ البوليفينيل كحول (CS/PVA) بنسب وزنية مختلفة (2:98، 4:96، 6:94، 8:92، و10:90%) باستخدام طريقة الصب بالمحلول لدراسة الخصائص البنيوية والحرارية وقوة الشد للمركبات. أظهرت مطيافية الأشعة تحت الحمراء بتحويل فورييه (FTIR) لعينات CS/PVA بعض الاختلافات، مثل التغيرات في قوة وموقع وشدة نطاقات تمدد CO₂ وCH₂ وكشفت المسعرة التفاضلية الماسحة (DSC) أن إضافة PVA حسنت الاستقرار الحراري للمركبات، حيث سجلت نسبة 2:98 أعلى درجة انصهار (T_m) عند 289 درجة مئوية. أكد التحليل الحراري الوزني (TGA) تحسن الثبات الحراري، حيث أظهر تحولاً ملحوظاً في ذروة التحلل نحو درجات حرارة أعلى، وانخفاضاً في فقدان الكتلة ضمن منطقة التحلل (فقدان ما يقارب 40% من الوزن بين 250 و400 درجة مئوية). ميكانيكياً، أظهر مزيج الكيتوزان/بوليفينيل الكحول بنسبة 2/98 وزنياً أداءً مثاليًا، محققاً قوة شد تبلغ 54.94 ميغا باسكال، واستطالة عند الكسر تبلغ 3.93%، ومعامل يونغ يبلغ 1.48 جيغا باسكال. أظهر الفحص المجهر الإلكتروني الماسح (SEM) توزيعاً متجانساً للغاية لبولي فينيل الكحول داخل الكيتوزان عند هذه النسبة المحددة، وهو ما يرتبط ارتباطاً مباشراً بقوة الشد الفائقة والمرونة المحسنة للمركب.

الكلمات المفتاحية: الكيتوزان، الخلائط، بولي فينيل الكحول، متانة الشد، التحلل الحراري.